Transparent miniature dielectric resonator for electron paramagnetic resonance experiments

Aharon Blank, Eli Stavitski, Haim Levanon, and Firdus Gubaydullin

Related Articles

Terahertz scattering by two phased media with optically soft scatterers
J. Appl. Phys. 112, 113112 (2012)

A single coil radio frequency gradient probe for nuclear magnetic resonance applications
Rev. Sci. Instrum. 83, 124701 (2012)

GaP based terahertz time-domain spectrometer optimized for the 5-8 THz range
Appl. Phys. Lett. 101, 181101 (2012)

On the performance enhancement of adaptive signal averaging: A means for improving the sensitivity and rate of data acquisition in magnetic resonance and other analytical measurements
Rev. Sci. Instrum. 83, 105108 (2012)

Terahetz detection by heterostructed InAs/InSb nanowire based field effect transistors
Appl. Phys. Lett. 101, 141103 (2012)

Additional information on Rev. Sci. Instrum.

Journal Homepage: http://rsi.aip.org

Journal Information: http://rsi.aip.org/about/about_the_journal

Top downloads: http://rsi.aip.org/features/most_downloaded

Information for Authors: http://rsi.aip.org/authors

Transparent miniature dielectric resonator for electron paramagnetic resonance experiments

Aharon Blank, Eli Stavitski, and Haim Levanon[a]
Department of Physical Chemistry and the Farkas Center for Light-Induced Processes, The Hebrew University of Jerusalem, 91904 Jerusalem, Israel

Firdus Gubaydullin
Zavoisky Physical-Technical Institute, 10/7 Sibirsky trakt, Kazan 420029, Russia

A novel miniature ($\sim 2 \times 2 \times 1$ mm) dielectric resonator for X-band electron paramagnetic resonance experiments is presented. The resonator is based on a single crystal of $KTaO_3$, which is excited to its $TE_{01\delta}$ resonance mode by means of a simple iris-screw coupling. Several configurations of resonators are considered and discussed with respect to their filling factor, power conversion ratio, and optical excitation efficiency. Our findings are presented in terms of both experimental and theoretical studies. For small samples, the high filling factor of this resonator results in a signal increase by a factor of 140–800 (assuming nonsaturating conditions) as compared to a rectangular X-band cavity. The high power conversion factor (~ 40 G/$\sqrt{W}$), should enable one to perform pulse experiments employing power amplifiers, with ~ 100-fold less peak power used for rectangular cavities. With an antireflective layer, the crystal's transparency enables efficient laser illumination of the sample in light-induced experiments. © *2003 American Institute of Physics.*
[DOI: 10.1063/1.1568550]

I. INTRODUCTION

Electron paramagnetic resonance (EPR) spectroscopy employs microwave (MW) frequencies to reveal many important aspects of paramagnetic materials.[1] One of the key factors, which determine the sensitivity of this method, is the MW resonator in which the paramagnetic sample is placed. In the EPR experiment, the signal intensity is directly proportional to the quality factor of the resonator, Q, the filling factor of the sample in the resonator, η, and the square root of the MW power, P.[1]

$$\text{EPR signal intensity} \propto \eta Q \sqrt{P}. \qquad (1)$$

Another important property of the resonator is its power conversion factor, C_p, which is defined as the ratio between the MW magnetic flux density in the resonator, B_1, and the power entering the resonator, which is given by

$$C_p = B_1 / \sqrt{P}. \qquad (2)$$

High C_p implies that for a given B_1, the required power from the amplifier is relatively low.

Different types of resonators have been described in the literature of which we should mention rectangular and cylindrical cavities,[1] loop-gap (or split-ring) resonators,[2–6] and dielectric resonators.[7–9] Each type has its own advantages and disadvantages in terms of size, cost, magnetic field homogeneity, filling factor, quality factor, and power conversion factor. Moreover, the resonator of choice strongly de-

pends upon the specific EPR experiment, i.e., continuous-wave (cw) or pulsed modes and the corresponding time-resolved EPR (TREPR) experiments.[10,11]

In this article, we present a new resonator, which can be applied in cw, pulsed, or cw-TREPR experiments. This resonator increases significantly the EPR signal intensity and allows performing pulsed experiments with much lower MW power requirements than the current designs. The resonator employs a material possessing high dielectric constant (permittivity, i.e., $\varepsilon_r = \varepsilon' - i\varepsilon''$) accompanied by low dielectric losses, and transparency in the visible region. We will present several configurations of this resonator, placed in a metallic shield, and analyze in detail its MW properties.

II. CHARACTERISTICS OF DIFFERENT RESONATORS: OUTLOOK

Most EPR resonators are made of metallic structures, whose dimensions correspond to the required resonance frequency. Unlike the metallic configurations, the dielectric resonator (DR) is a MW device, made of a material of high dielectric constant with low dielectric losses.[12] Early designs of dielectric resonators were based upon materials with a relative dielectric constant $|\varepsilon_r| < 10$ (e.g., fused silica and alumina).[7] More advanced designs, utilizing the progress in material science, resulted in the construction of resonators made of ceramics (tin-zirconium tetra-titanate) with a dielectric constant of ~ 38.[8] With small DRs, the sample volume can be decreased, without affecting the filling factor of the resonator and the sensitivity of the measurement. For example, in X band (10 GHz), the active volume of a rectangular metallic cavity is ~ 1–10 cm^3;[1] for a loop-gap resonator it may be as small as 0.1 cm^3;[6] and for a DR, with ε_r
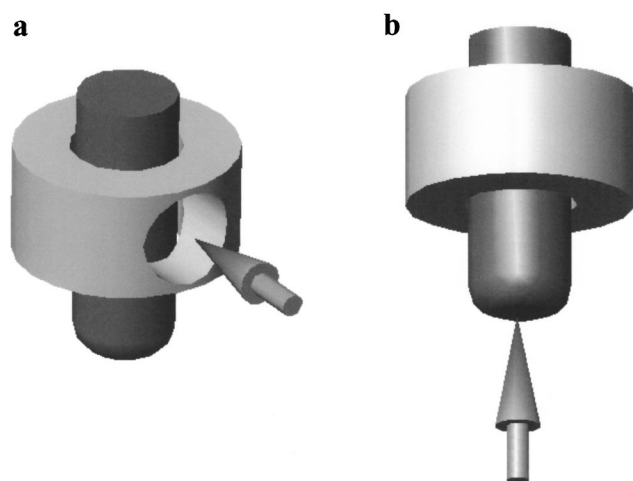
a   **b**

FIG. 1. (a) Illumination of a sample inside a nontransparent dielectric ring from the side, through a hole drilled in the ring. (b) Illumination of the sample from the bottom.

FIG. 2. Schematic layout of the resonator based on the $KTaO_3$ resonator (two cuts and isometric view, into the resonator body). In the upper-right inset, a larger view of the resonator ring (with the sample in it), in single and double-stacked configurations, is shown.

$=38$, it may be even smaller than 0.008 cm^3. The second advantage is the high quality factor of the DR, which can be as high as 5000 (without the sample, critically coupled), but can be much lower by overcoupling the resonator, an important requirement for pulsed experiments.[10] An additional advantage of DRs is their high power conversion factor, C_p [Eq. (2)], which is usually ~ 5 G/$\sqrt{W}$ (similar to loop-gap resonators[4]), as compared to ~ 1 G/$\sqrt{W}$ for rectangular metallic cavities.[6,13,14] In pulsed experiments, in which short (~ 10 ns) intense MW pulses are applied, high C_p is important and should lead to relatively low power requirements. Finally, unlike the loop-gap resonators or rectangular cavities, the DR is characterized by a better separation of the electric from the magnetic fields, confined to the sample volume, thus decreasing the possible dielectric losses.

In contrast to these important and valuable advantages, there are several difficulties when performing cw-TREPR measurements associated with DRs in conjunction with light induced transient phenomenon. The first difficulty is the relatively high Q of DRs (when critically coupled), which limits the time resolution of the detection. Thus to obtain a time resolution of ~ 10 ns in X band, Q must be lowered to ~ 300 by inserting a substance with high dielectric losses near the resonator, e.g., H_2O. This problem does not exist at higher frequencies, e.g., at W band (94 GHz), where even for very high Q, time resolution, estimated as $\sim Q/\omega_0$, is in the order of 10 ns or less. An additional difficulty is related to the illuminated filling factor, η_L (the filling factor of the volume that can be photoexcited) as opposed to the filling factor of the entire sample, η.[15,16] In regular pulsed- or cw-EPR experiments of stable paramagnetic species, the EPR signal is proportional to η. However, in light induced experiments, only the illuminated part, where the transient paramagnetic species are formed, is relevant to the signal detection. The ceramic DRs, with high dielectric constants and low dielectric losses, are not transparent to visible light, facing difficulties in efficient illumination of the sample volume inside the resonator. Figure 1 presents two possible geometries for illumination of the sample in the ceramic ring. One possibility is
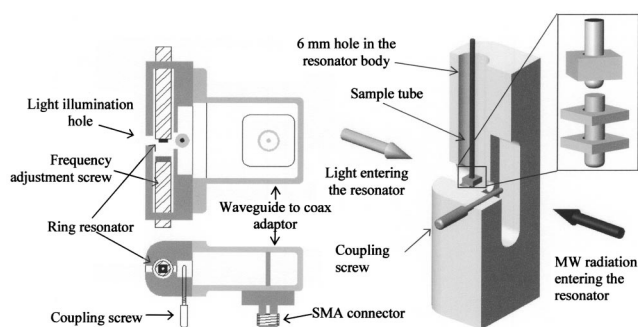
photoexcitation through a hole drilled in the ceramics [Fig. 1(a)]. This solution is problematic, since a large hole decreases significantly the Q of the resonator and distorts its $TE_{01\delta}$ mode.[17] Thus one is forced to reduce the diameter of the hole and decrease the volume of the sample that can be illuminated. The difficulty of inefficient illumination also occurs with loop-gap resonators, where only a small fraction of the entire sample's volume in the resonator can be exposed to the photoexcitation.[6] Moreover, we have found that illumination of the small sample (less than 2 mm in diameter) from the bottom [Fig. 1(b)] is also inefficient, reducing significantly the signal intensity. Another approach to enable efficient light excitation is to employ a double-stacked DR[9] (cf., Fig. 2 and see below), where the illuminated sample is placed between two dielectric rings. However, the magnetic field, B_1, between the rings is lower than that inside the rings, thus reducing η_L with respect to the overall filling factor, η, of the resonator. The problems of light illumination can be circumvented using DRs made of transparent materials. As it stands now, sapphire, with a dielectric constant of ~ 10, is used commercially as a resonator, enabling sufficient optical transparency. However, the relatively low dielectric constant of this material corresponds to relatively large dimensions of the resonator, meaning that the active volume required to be illuminated is relatively large, i.e., ~ 0.2 cm^3.

In this article, we present several new designs employing a ferroelectric[18] resonator made of a single crystal of $KTaO_3$ with a dielectric constant of ~ 230, at room temperature, excited to its $TE_{01\delta}$ mode at X band (see discussion below). This material, when optically polished, is transparent in the visible region, allowing efficient photoexcitation of the sample. The use of similar ferroelectric crystals, to increase the EPR sensitivity, was discussed recently.[19,20] All these studies present a simple structure in which a hollow cylinder of $KTaO_3$ is placed inside a regular rectangular metallic cavity and causes a dramatic increase in the EPR signal intensity for small samples. This increase is due to redistribution of the magnetic fields and increase in the filling factor. A similar configuration, with a $ZrSnTiO_4$ dielectric ring having ε_r ~ 38 was also discussed recently.[21] The problem with such designs is that the coupling of the microwaves to the resonator occurs indirectly by the TE_{102} resonance mode of the rectangular metallic cavity, without really exciting the $TE_{01\delta}$
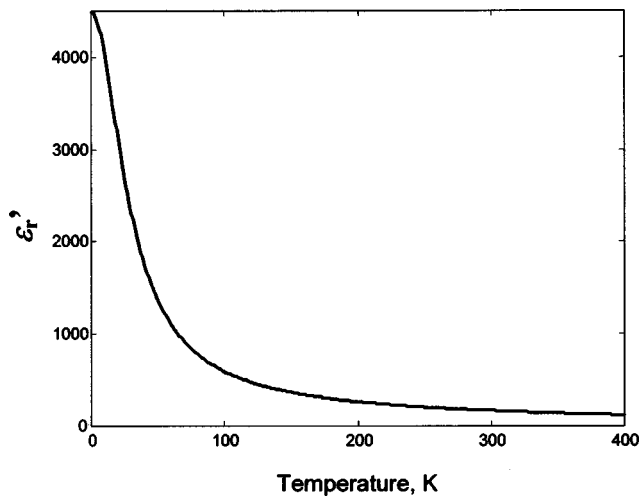
FIG. 3. ε_r' vs temperature for a single crystal of KTaO$_3$ (see Ref. 23).

FIG. 4. Optical density of a polished single crystal of KTaO$_3$ (1 mm thickness). The spectrum was measured using an HP8453 spectrophotometer.

ring resonance mode.[22] Since the latter resonance mode is not excited, one cannot obtain very high magnetic fields inside the resonator. Therefore the advantages of a KTaO$_3$ crystal in terms of filling and conversion factors are not fully exploited. In addition, the configuration where the KTaO$_3$ crystal is placed in a TE$_{102}$ cavity is susceptible to a noticeable temperature dependence of the EPR signal intensity. This is probably due to change in the permittivity of the crystal, which changes the coupling properties of the TE$_{102}$ mode.[19]

III. TECHNICAL DESCRIPTION

The basic layout of the present resonator and its coupler, operating at X band, is illustrated in Fig. 2. Similar devices can be operated at higher or lower frequencies by an appropriate scaling of the resonator's dimensions. The system consists of the following components: a: the main body; b: the ferroelectric ring resonator; c: the coupling iris and screw; d: the optical window; e: the frequency adjustment screw; and f: the waveguide to a coax adaptor. We focus now on each component separately.

a: The main body is made of a brass cylinder with a 6 mm diameter hole drilled along the cylinder. This structure supports the Teflon screws holding the resonator and the frequency varying screw. It also functions as a Faraday cage to reduce radiation from the resonator. To maintain high Q of the resonator, the inner side walls of the main body should be gold plated and have minimal surface roughness, the machining procedure should be made with electroerosion.

b: The ring resonator is made of a single crystal of potassium tantalite (KTaO$_3$), which is commercially available (e.g., Commercial Crystal Laboratories Inc., Segeisa Inc.). The raw material is supplied as a flat plate and then it can be cut by a diamond disk and drilled with a diamond drill. The dimensions of our X-band resonator are $2.2 \times 2.2 \times 1$ mm, with a 1 mm hole diameter. KTaO$_3$ has a dielectric permittivity (ε_r), which depends upon temperature and frequency, and the theoretical temperature dependence is plotted in Fig. 3.[23] As indicated earlier, at room temperature, which is well above the Curie temperature of this crystal (32.5 K), this
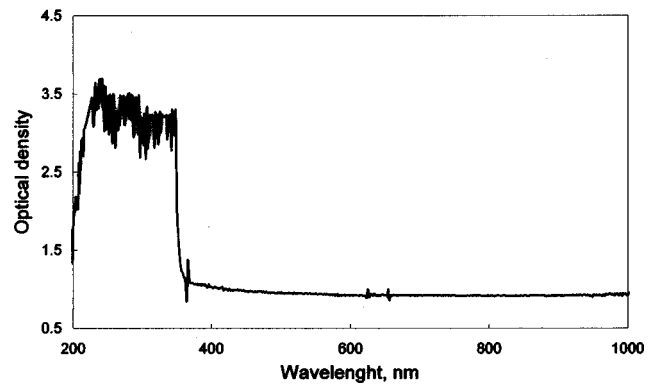
material is paraelectric, exhibiting a typical change in ε_r of $\sim$0.37% per degree. The frequency dependence of the permittivity of this crystal (not shown) is relatively large in the lower frequency range (below $\sim$1 MHz), but around X band, the dependence is much smaller.[24] The crystal losses are defined by its $\tan\delta (=\varepsilon''/\varepsilon'=1/Q)$ value and the crystal can be supplied with various $\tan\delta$, depending on the specific method of crystal growing. Thus crystals with low losses, e.g., $\tan\delta = 6 \times 10^{-4}$ at room temperature,[23] can be used as resonators, suitable for cw, or low time resolution (cw-TREPR) measurements. Crystals with high losses can be chosen for high time resolution (cw-TREPR) or pulsed EPR measurements. We have also found that fast cooling of the crystal to 77 K may generate defects, which cause an increase of its losses. However, slow heating of the crystal to $\sim$950 °C, for several hours under O$_2$ atmosphere, reduces its losses by an annealing. Annealing should also eliminate defects, which can be generated in the crystal during the machining processes. With respect to optical properties, Fig. 4 indicates that the crystal is almost transparent in the visible region. However, for efficient photoexcitation, the ring resonator should be polished in the inner and outer parts. Moreover, the high index of refraction of this crystal ($\sim$2.28 and Fig. 4)[25] require an antireflective (AR) layer to coat at least one side of the polished faces. This will reduce the light reflection from the crystal/air interface.

c: The part, which consists of the coupling iris and screw, couples the MW energy from the waveguide to the ring resonator and enables one to match it to the impedance of the transmission line. The orientation of the coupling screw is chosen to excite efficiently the TE$_{01\delta}$ mode of the ring resonator.

d: The optical window is a hole drilled in the main body. The diameter of the hole should be $\sim$2 mm.

e: The frequency adjustment screw made of Teflon is attached to a thin cylindrical brass plate. It serves as a frequency-adjustment device. The resonance frequency of the ring increases as the brass plate approaches it. In the present design, the frequency can be tuned in a range of $\sim\pm75$ MHz about the center frequency of the resonator, without affecting significantly the coupling properties and the quality factor Q. A typical experimental plot, describing the resonance frequency versus distance of the ring from the
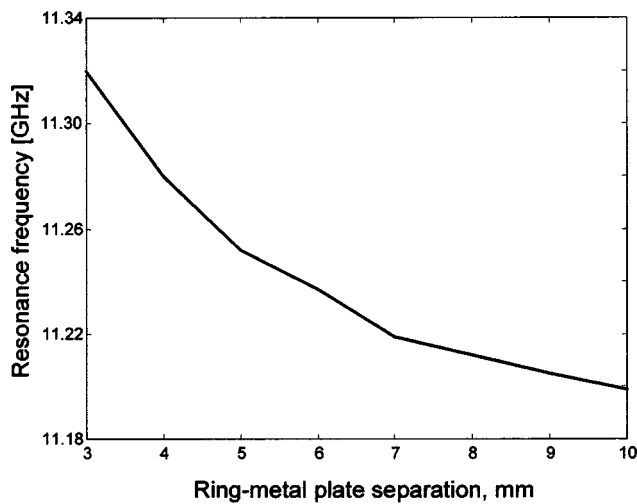
FIG. 5. Measured resonance frequency vs the distance between the resonator ring and the metal plate (for a single ring resonator configuration).
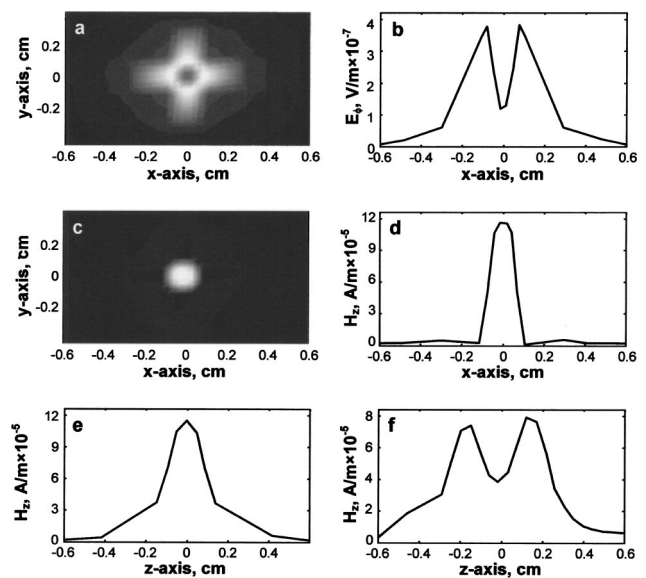

FIG. 6. Calculated fields for single and double-stacked ring resonators excited to their $TE_{01\delta}$ mode. The fields are defined in a cylindrical coordinate system, the z axis is along the sample (see Fig. 2). The dimensions of the resonators are $2.2 \times 2.2 \times 1$ mm, with a central hole of 1 mm diameter and a separation of 1 mm between the rings for a double-stacked configuration. (a) Two-dimensional image of the electric field (E_ϕ) along the central xy plane of a single ring resonator; (b) same as (a) but plotted along the x axis of the ring resonator; (c) two-dimensional image of magnetic field (H_z) along the central xy plane of a single ring resonator; (d) the same as (c) but plotted along the x axis of the ring resonator; (e) same as (c) but plotted along the z axis of the resonator; and (f) plot of H_z along the z axis of the double-stacked resonator. Notice that at the center of the resonator, where light excitation takes place, the field is ~ 3 times smaller than for a single ring resonator. (a)–(d) are valid fields for a double-stacked resonator in terms of qualitative behavior.

metal plate is shown in Fig. 5. In the case of a double-stacked dielectric resonator structure, the frequency can be varied by changing the distance between the rings,[9] leading to a larger frequency tuning capability (~ 500 MHz). In our experiments, employing a double-stacked configuration, the distance between the two rings was kept fixed (1 mm).

f: The current design relies on the excitation of the ring resonator through a regular rectangular metal waveguide. Our MW source output comes from a coaxial connector; therefore an integral part of this system is the waveguide-to-coax adaptor, which is positioned just before the coupling iris of the resonator (cf., Fig. 2).

IV. THE CHARACTERISTICS OF THE RESONATOR

In this section we discuss in detail the important characteristics of the present resonator. The magnetic and electric fields inside the resonator were calculated using a numerical procedure (finite element method).[15] Figure 6 presents results of such a calculation, showing that the magnetic fields at the center of the resonator are very strong, and that they are well separated from the electric fields, confined to the resonator's body. These results are typical for the $TE_{01\delta}$ mode of the ring resonance.[26] A similar calculation was performed for a double-stacked resonator structure [Fig. 6(f)].[9] Inspection of Figs. 6(e) and 6(f) shows that a separation larger than ~ 1 mm between the rings results in a substantial drop of the magnetic fields between the rings, thus reducing the filling factor. This is due to the high permittivity of the crystal employed. It should also be noted that in order to maintain a stable $TE_{01\delta}$ mode, the single ring resonator height should be less than the ring's radius (or half the length of the square, in our case).[26]

The operational frequency for a given dielectric structure cannot be calculated analytically. However, an approximate expression provides, within $\sim 10\%$ accuracy, the estimated resonance frequency of the resonator:[26]

$$f_{GHz} = \frac{34}{a_{mm}\sqrt{\varepsilon_r}}\left(\frac{a}{h} + 3.45\right), \tag{3}$$

where a is the radius of the dielectric ring (in mm) and h is the height of the ring. For our resonator, with a rectangular cross section, one may use the half of the smaller side of the rectangle ($a = 1$ mm) and obtain a frequency, $f \sim 10$ GHz. A much more accurate calculation employs the numerical approach of the finite element solution of the fields of the resonator (cf., Fig. 6).[15,16] The numerical approach also accounts for the distance of the resonator from the metal walls of the main body structure, which tends to increase the resonance frequency, as the structure becomes smaller (Fig. 5). As mentioned above, the permittivity of the crystal exhibits strong temperature dependence, especially at very low temperatures (Fig. 3). This dependence should probably prevent the operation of this resonator below ~ 150 K. Nevertheless, at room temperature, a $1°$ change would result in an ~ 18 MHz change in the resonance frequency of the resonator. Such fluctuations can easily be compensated with the automatic frequency control circuit, which is an essential part of any EPR spectrometer.

In our current design, using crystals from two different sources, we have found that both crystals gave similar results with respect to their loaded quality factor, which was measured to be $Q_L \sim 1150$. Q_L was measured at the critical coupling without any sample in the resonator, using a homebuilt network analyzer. The measurements were carried out by finding the ratio between the resonance frequency and linewidth of the resonator's reflection coefficient, measured at -3 dB from the baseline, of the dip.[26,27] Thus, assuming that
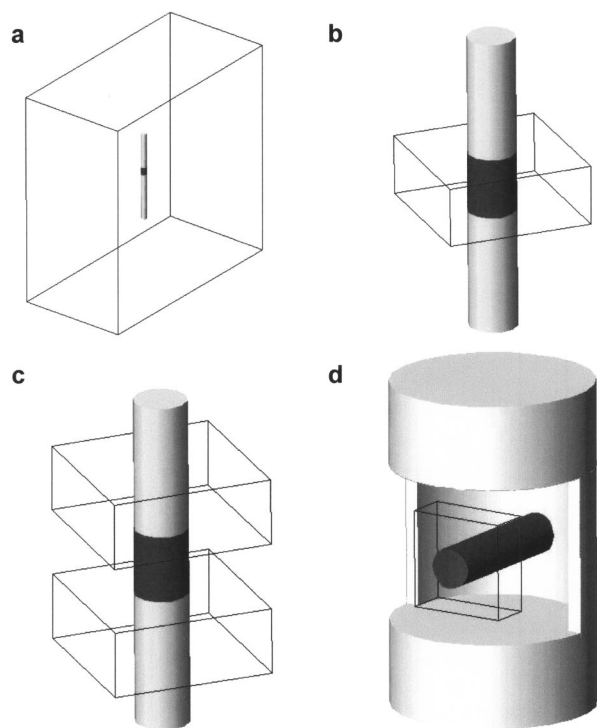
FIG. 7. Several possible configurations for filling factor calculation. In cases (a)–(c) a thin Pyrex tube (o.d. 1 mm and i.d. 0.8 mm) is used to contain the sample (represented by the gray cylinder). (a) The sample is placed inside a TE_{102} rectangular X-band cavity ($10\times22\times41$ mm). The filling factor of the illuminated region by a 1 mm laser spot (marked by the black cylinder) is calculated to be 1.1×10^{-4}; (b) the sample is placed inside the ferroelectric resonator ($2.2\times2.2\times1$ mm). The filling factor of the illuminated region is 0.135; (c) the sample in a double-stacked resonator with dimensions as in (b) (ring separation is 1 mm). The filling factor of the illuminated region is 0.038; (d) the resonator ring is placed inside the sample tube, thus enabling efficient illumination of a large volume. Notice that, unlike case (b), light does not pass through the crystal. The filling factor of the illuminated region is 0.18. If we assume the use of a large laser spot, or, for the case of a stable radical, measured by cw or pulsed EPR, the filling factor of this configuration is >0.8.

the losses in the metal body are negligible, the Q of the crystal itself was calculated to be ~2300. We found that when the crystal was cooled rapidly to 77 K and heated back slowly to room temperature, its Q_L dropped down to ~500. Such cooling process may be of importance when performing high time resolution cw-TREPR measurements, which require low Q_L.

One of the most important properties of the described resonators is their high filling factor for very small samples, especially in light induced experiments. The filling factors of the various resonators, based upon the $KTaO_3$ ring, were calculated by the numerical method described above.[15,16] Figure 7 presents different configurations and the calculated results for the illuminated filling factor, η_L (discussed above[15,16]). As compared to a "conventional" rectangular cavity (a), the illuminated filling factor increases by 280–1600, depending on the exact structure of the resonator. Since Q_L of the ring resonator is ~2 times smaller than that of a rectangular cavity (measured to be ~2200 in our case), the corresponding overall increase in EPR signal should therefore be ~140–800 [cf., Eq. (1)].[28]
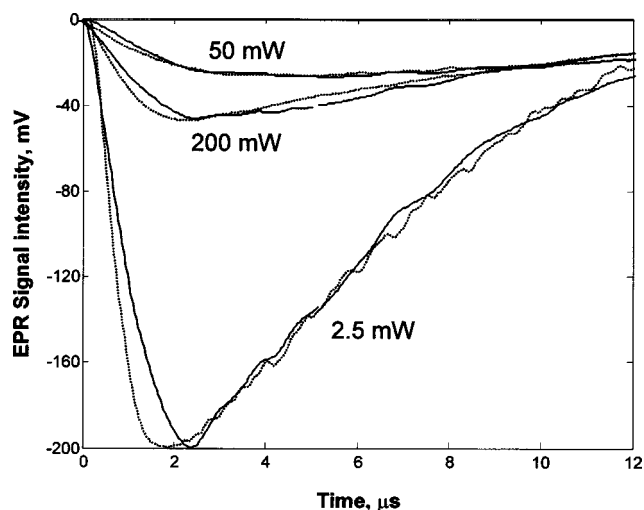

FIG. 8. cw-TREPR signal intensity as a function of time after laser excitation. Dotted line: experimental results; solid line: theoretical curve using Eq. (4). The two upper traces show the weak signal from the sample in a rectangular cavity with relatively high MW power excitation. The lower trace shows the strong EPR signal in the double-stacked resonator, with relatively low MW power excitation.

The power conversion factor of the present resonator was measured by comparing the kinetic curve in a cw-TREPR experiment, performed with a standard commercial rectangular cavity (Varian model V-4531), with that obtained using a double-stacked resonator. The kinetic curve was that of polarized radical (deuterated BDPA, alpha, gamma-bisdiphenylene-β-phenylallyl) generated via the photochemical reaction between a photoexcited triplet chromophore and a stable radical. For the detailed experimental procedure and theoretical background, the reader is referred to earlier publications.[29] For a time-dependent magnetization, $M(t)$, the corresponding signal kinetics in a cw-TREPR experiment is given by[30]

$$M_y(t)\propto M(t)\cdot\frac{\omega_1 e^{at}}{b}\sin(bt);$$

where

$$a=-\frac{1}{2}(T_1^{-1}+T_2^{-1});\quad b=\left[\omega_1^2-\frac{1}{4}(T_2^{-1}-T_1^{-1})^2\right]^{1/2}. \quad (4)$$

Here we assumed that most of the signal results from polarized (non-Boltzmann) spin population. In Eq. (4) $\omega_1 = \gamma B_1/2\pi$, where γ is the electron gyromagnetic ratio; and T_1 and T_2 are the spin-lattice and spin-spin relaxation times of the radical, respectively. Therefore by performing the same experiment at different MW powers, using the same sample, with the different resonators, i.e., the rectangular cavity and the double stacked resonator, the procedure allows one to extract the ratio between C_p of the corresponding resonators. Figure 8 presents the results of such an experiment. The experiments were performed with a Varian E-12 spectrometer, and with both resonators, similar sample volume was illuminated using a small diameter laser beam <2 mm (Lightwave 210 Nd:YAG laser). Fitting of the kinetic curves [Eq. (4)] was carried out with known parameters, T_1 and T_2, leaving ω_1 as a fitting parameter. Such a fitting (Fig.

8) corresponds to a power conversion factor of $C_p = 1.4$ and $13\ G/\sqrt{W}$ for the rectangular and double-stacked resonator, respectively.

At this stage we can estimate C_p of a single ring resonator to be ~ 3 times larger than that of a double stacked one. This figure is based on the calculated magnetic fields in the double-stacked resonator [Fig. 6(f)], as compared to the fields of a single ring resonator [Fig. 6(e)]. In addition, a ratio of ~ 3 in the magnetic field intensity was also found for single and double-stacked resonators employing $ZrSnTiO_4$ ceramics with $\varepsilon_r = 38$.[9] Therefore the conversion factor for a single ring resonator is $\sim 40\ G/\sqrt{W}$ versus $1.4\ G/\sqrt{W}$ in the rectangular cavity. The value obtained for the rectangular cavity is in reasonable agreement with a prior report of C_p for rectangular cavities.[6,13,14]

One of difficulties in using the $KTaO_3$ single crystal is associated with its background EPR signal. In the cw-TREPR experiments, we are mainly concerned with transient signals, and the background signal is easily eliminated. Nevertheless, in cw or pulsed experiments the background signal problem may arise. At room temperature, the background signal (mainly due to Fe^{3+} impurities) is broad because of fast relaxation processes in the crystal.[31] At low cryogenic temperatures, the signal becomes very sharp and very anisotropic.[32] Any measurement procedure subjected to this background signal should include a proper subtraction of this signal before sample insertion. In most resonators, such a subtraction process is problematic because upon removal of the sample from the resonator, its resonance frequency and Q changes, thus affecting the EPR signal. In the present resonator, however, the subtraction is less problematic due to the high permittivity of $KTaO_3$, resulting in good E-to-H field separation, i.e., very small change in the resonance frequency and Q upon sample insertion.

The predicated increase in EPR signal intensity was already discussed above with respect to the resonator's filling factor. The results given in Fig. 8 show the signal increase in our resonator. When analyzing these results, we see that the obtained signal is ~ 4.6-fold stronger in the double-stacked resonator than in the rectangular cavity, for the same illuminated sample volume. However, the signal in the double-stacked resonator was obtained with much lower MW power (2.5 mW as compared to 200 mW). Thus, considering Eq. (1), we obtain that for the same power and sample size, the increase in EPR signal using the double-stacked resonator is ~ 41 as compared with the rectangular cavity. This increase is still about three times smaller than the predicted results, based on the filling factor calculation (see above). We believe that the relative reduction in the EPR signal intensity in the double-stacked resonator, as compared to theory, is the result of two main factors. The first is due to the laser spot size (< 2 mm), which extends beyond the 1 mm gap of the double-stacked rings, and did not penetrate well inside the rings due to the high refractive index of the $KTaO_3$ crystal (we did not employ an AR layer, see above). The second reason is due to the required detuning process performed in our spectrometer (Varian). In more detail, after the cavity is critically matched, it is detuned a bit to supply the detection diode with a power bias (~ 1 mW) to obtain detection in the linear region of the diode.[33] When this detuning is performed at relatively high power output, it does not change significantly the resonator's matching from critical coupling and, therefore, the signal is maximum.[1] When the output power is very low, e.g., ~ 2.5 mW in our case, the detuning process can greatly reduce the EPR signal as the resonator is far from critical coupling. Unfortunately, due to the high conversion factor of our resonator and the relatively small linewidth of the radical, we could not increase the power above ~ 2.5 mW without losing too fast the signal due to strong saturation. It should be noted that by employing a different chemical system with a larger radical linewidth, the signal will escape detection using the small sample in the large rectangular cavity.

Another possible difficulty is the background laser spike. This signal may reduce the sensitivity of the measurement, even though the EPR signal increases.[6] We have found that the background laser spike did not increase when changing from a rectangular cavity to a double-stacked resonator. This is probably due to the fact that in the double stacked resonator only the sample region was illuminated without hitting the metal walls.

ACKNOWLEDGMENTS

[1] C. P. Poole, *Electron Spin Resonance: A Comprehensive Treatise on Experimental Techniques*, 2nd ed. (Dover, New York, 1997).
[2] M. Decorps and C. Fric, J. Phys. E **5**, 337 (1972).
[3] W. N. Hardy and L. A. Whitehead, Rev. Sci. Instrum. **52**, 213 (1981).
[4] W. Froncisz and J. S. Hyde, J. Magn. Reson. (1969-1992) **47**, 515 (1982).
[5] W. Froncisz, T. Oles, and J. S. Hyde, Rev. Sci. Instrum. **57**, 1095 (1986).
[6] G. Elger, J. T. Törring, and K. Möbius, Rev. Sci. Instrum. **69**, 3637 (1998).
[7] J. L. Harthoorn and J. Smidt, Appl. Sci. Res. **20**, 148 (1969).
[8] R. Dykstra and G. Markham, J. Magn. Reson. (1969-1992) **69**, 350 (1986).
[9] A. Sienkiewicz, K. Qu, and C. P. Scholes, Rev. Sci. Instrum. **65**, 68 (1994).
[10] M. K. Bowman, *Fourier Transform Electron Spin Resonance* (Interscience, New York, 1990).
[11] L. T. Muus, P. W. Atkins, K. A. McLauchlan, and J. B. Pedersen, *Chemically Induced Magnetic Polarization* (Reidel, Dordrecht, 1977).
[12] D. Richtmyer, J. Appl. Phys. **10**, 391 (1939).
[13] Y. E. Nesmelov, J. T. Surek, and D. D. Thomas, J. Magn. Reson. (1969-1992) **153**, 74 (2001).
[14] Bruker Biospin GmbH, User manual for the Bruker ESP380E system.
[15] A. Blank and H. Levanon, Spectrochim. Acta, Part A **56**, 363 (2000).
[16] A. Blank and H. Levanon, Spectrochim. Acta, Part A **58**, 1329 (2002).
[17] A. Blank and H. Levanon, Appl. Phys. Lett. **79**, 1694 (2001).
[18] $KTaO_3$ possesses ferroelectric properties only below 32.5 K (namely, it exhibits spontaneous electric polarization). Thus at our working temperatures (about room temperature) this material is actually paraelectric (its electric dipoles behave under electric field in an analogous manner to magnetic dipoles under magnetic field in paramagnetic materials). Nevertheless, it is customary in the literature to refer to this material as ferroelectric.

[19] I. N. Geifman, I. S. Golovina, V. I. Kofman, and E. R. Zusmanov, Ferroelectrics **234**, 81 (1999).

[20] I. N. Geifman, I. S. Golovina, E. R. Zusmanov, and V. I. Kofman, Tech. Phys. **45**, 263 (2000).

[21] S. Del Monaco, J. Brivati, G. Gualtieri, and A. Sotgiu, Rev. Sci. Instrum. **66**, 5104 (1995).

[22] Reference 13 claims to design the resonators dimensions to support the $TE_{01\delta}$ resonance mode exactly at the resonance frequency of the rectangular cavity. This statement confronts several problems: (1) The mapping of the magnetic field along the insert (Ref. 13) clearly does not correspond to the $TE_{01\delta}$ mode (Ref. 26); (2) As discussed here, the resonance frequency of $KTaO_3$ is strongly dependent on temperature, making it unlikely to match exactly the two resonance frequencies even when small changes in temperature are considered; and (3) The increase in EPR signal intensity reported in Ref. 13 ($\sim$80) indicates that no efficient $TE_{01\delta}$ mode was excited. This is supported by our estimates of signal increase ($\sim$800) in our $TE_{01\delta}$ resonator versus rectangular cavity.

[23] O. G. Vendik, L. T. Ter-Martirosyan, and S. P. Zubko, J. Appl. Phys. **84**, 993 (1998).

[24] M. Dong and R. Gerhard, in *Frequency and Temperature Dependence of the Dielectric Properties of Ferromagnetic Materials* (IEEE New York, 1998), p. 327.

[25] J. Y. C. Wong, L. Zhang, G. Kakarantzas, P. D. Townsend, P. J. Chandler, and L. A. Boatner, J. Appl. Phys. **71**, 49 (1992).

[26] D. Kaifez and P. Guillon, *Dielectric Resonators*, 2nd ed. (Noble, Atlanta, 1998).

[27] The quality factor can be controlled during crystal manufacture (we requested the highest possible Q).

[28] Inspection of Fig. 7 shows that the largest increase in the EPR signal occurs when the ring resonator is inside the sample tube. This interesting, novel, and very efficient configuration can be obtained for liquid samples by using a relatively large sample tube (i.d. $\sim$3 mm) where the ring resonator is inserted inside the sample tube, prior to the sample preparation process. However, we have found in our experiments that when the solvent has high dielectric losses, such configuration may result in the decrease of Q. This is probably due to the strong electric field component, which exists outside our rectangular ring resonator (cf., Fig. 6).

[29] A. Blank and H. Levanon, J. Phys. Chem. A **105**, 4799 (2001).

[30] P. J. Hore and K. A. McLauchlan, Rev. Chem. Intermed. **3**, 89 (1979).

[31] B. Salce, J. L. Gravil, and L. A. Boatner, J. Phys.: Condens. Matter **6**, 4077 (1994).

[32] M. D. Glinchuk, V. V. Laguta, I. P. Bykov, J. Rosa, and L. Jastrabik, Chem. Phys. Lett. **232**, 232 (1995).

[33] In the last models of the Bruker spectrometers, there is usually a reference MW arm, which biases the detection diode without using the reflected power from the cavity.